PEER REVIEWED

Development of Ti6AlFe Alloy and its Microstructural Transformation During Synthesis and Subsequent Thermo-Mechanical Treatment

Ayad Omran Abdalla[1] · Astuty Amrin[2] · Khairur Rijal Jamaludin[2] · Meysam Toozandehjani[3]

Abstract

A compositional modification was initially carried out in Ti-6Al-4V alloy by substitution replacement of vanadium (V) by iron (Fe) as a β-stabilizing alloying element in order to develop Ti6Al(1-3)Fe alloys. Afterwards, Ti6Al(1-3)Fe alloys underwent rolling at 800 °C followed by solution heat treatment at 900 °C. Microstructural characterization reveals that Ti6Al(1-3)Fe alloys contain a lamellar α+β microstructure wherein size of lamellar colonies and the lamellae width gradually decrease by increasing Fe content. Subsequent thermo-mechanical and solution heat treatment lead to an increase in β-phase percentage by increasing Fe content. Ti6Al(1-3)Fe alloys show a superior hardness (HV), ultimate tensile strength (UTS) and elongation (%) owing to extensively refined lamellar α+β microstructure. HV values of Ti6Al(1-3)Fe alloys increase after thermo-mechanical treatment while UTS and elongation (%) values as well as corrosion properties drop due to the larger amount of β-phase in thermo-mechanical treated Ti6Al(1-3)Fe alloys.

Graphical Abstract
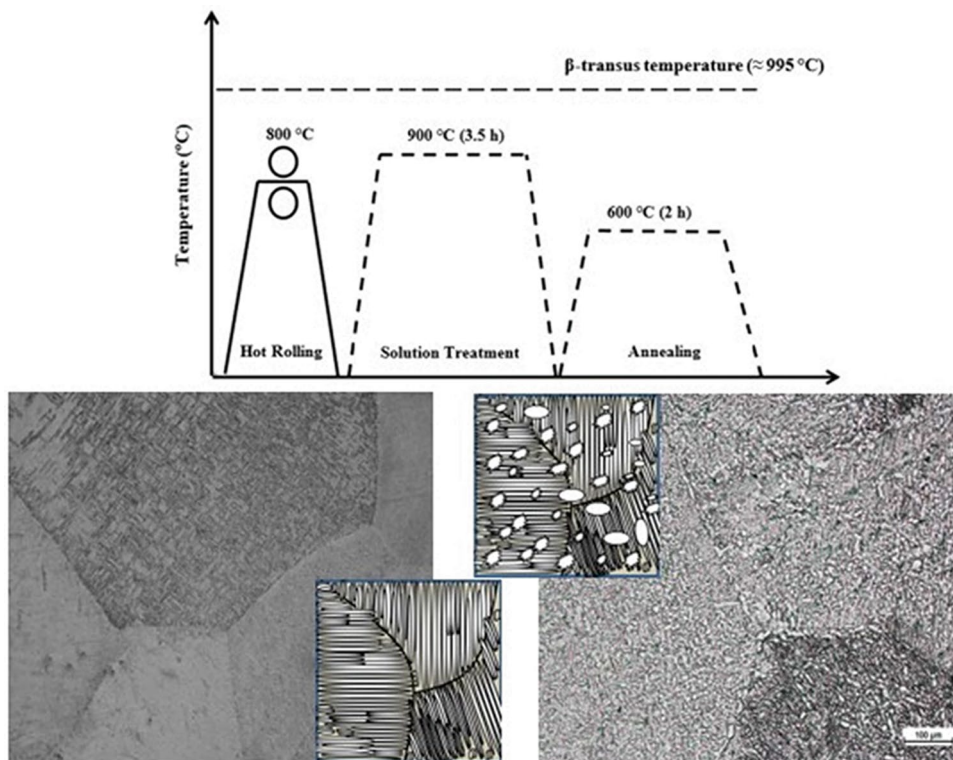
Extended author information available on the last page of the article

Introduction

Titanium alloy of Ti-6Al-4V is extensively utilized as a lightweight structural material for aerospace and automotive industries applications due to good combination of strength and ductility and in biomedical applications owing to outstanding corrosion resistance and biocompatibility [1–3]. However, this alloy is expensive due to the presence of expensive alloying elements like vanadium (V) which is widely used as a β-stabilizing element [4].

To lower the material cost and improve the properties simultaneously, researchers have introduced the cheaper alloying elements as an alternative to more expensive elements. The two phases (α+β) microstructure of Ti-6Al-4V can be easily modified and coherently affected by addition or altering the alloying elements and its composition. For example, Ti-4.5Al-6.8Mo-1.5Fe [5] and Ti-6Al-5Fe-0.05B-0.05C [6] have been developed by substituting B, C, Fe and Mo alloying elements instead of V. Fe is one of the attractive alloying elements to be added in Ti alloys [6–9]. Hideki and Kazuhiro [8] indicated that Fe can be used as an inexpensive alloying element in Ti-6Al-4V alloy to improve its mechanical properties and to lower its cost. Ti-Al-Fe alloy is also fully heat treatable where diversity of microstructures can be modified to optimize the mechanical properties [10]. Authors have also previously reported that substituting Fe as an β-stabilizing alloying element is able to alter microstructure of Ti-6Al-4V alloy [9–11].

Mechanical properties of Ti-6Al-4V are associated to two-phase (α + β) microstructure and significantly affected by the morphology, fraction, size, and distribution of phases. It is well known that two-phase (α + β) microstructure and subsequent mechanical properties are governed by thermomechanical treatments. The achievement of optimum properties including strength, ductility and corrosion properties is expected through suitable thermo-mechanical treatment [2, 12, 13]. Thermo-mechanical treatments are useful techniques for refinement of Ti-6Al-4V microstructure [3]. Thermo-mechanical treatments are used to control the morphology of α- and β- phases, to control α-phase size and to optimize α/β ratio which their adjustment subsequently results in enhancement of mechanical properties [3, 14, 15].

Therefore, the primary aim of this work was to modify the composition of Ti6Al4V alloy by substitution of V by Fe as a β-stabilizing alloying element in order to develop Ti6Al(1-3)Fe alloys. The second aim was to modify the microstructure of Ti6Al(1-3)Fe alloys by thermo-mechanical treatment including a combination of hot rolling and solution heat treatment. Finally, the effect of thermo-mechanical

treatment on the microstructural, mechanical and corrosion properties of Ti6Al(1-3)Fe alloys was investigated and compared to un-treated Ti6Al(1-3)Fe alloys.

Materials and Methods

Ti6Al(1-3)Fe alloys containing up to three weight percentage (wt.%) were manufactured by a vacuum arc melting. Vacuum arc melting was conducted using tungsten electrode in TIMET Co. (USA). Afterwards, Ti6Al(1-3)Fe alloys underwent thermo-mechanical processing in order to manipulate the microstructure as schematically presented in Fig. 1. Ti6Al(1-3)Fe alloys were plastically hot rolled at 800 ± 50 °C in the dual phase (α+β) region to obtain 35% thickness reduction and reach to desired thickness of 6 mm. The solution treatment was performed at 900 °C below β-transus (T_β) for 3.5 hours followed by water quenching. Then, specimens were annealed at 600 °C for 2 hours and cooled in the air. After completing the manufacturing process, surface of the specimens was treated by blasting and pickling and all sharp edges were grounded to obtain final dimensions of $160 \times 60 \times 6$ mm.

Before microstructural characterization, the surfaces of Ti6Al(1-3)Fe specimens were prepared following a standard metallographic procedure. The microstructural features of Ti6Al(1-3)Fe were observed using NIKON Eclipse optical microscope and Hitachi SU8020 FESEM. FESEM micrographs were taken in backscattered electron imaging (BSE) mode. NIS-Elements imaging analysis software was employed to measure microstructural features; the lamellae width and grain size. Thermal analysis was carried out using a TGA/DSC-1 (Mettler Toledo) to identify the β-transus
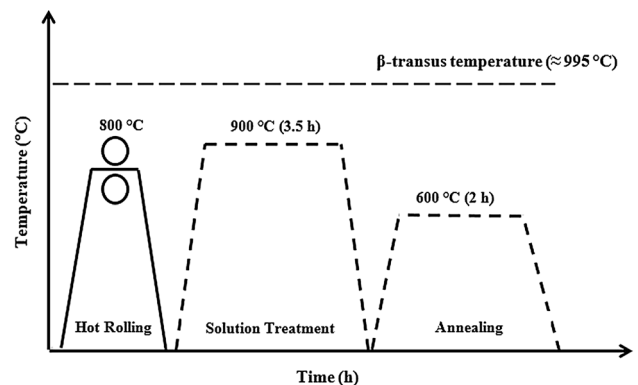

Fig. 1 Schematic diagram of thermomechanical and heat treatment used for Ti6Al(1-3)Fe Alloys

temperature in Ti6Al(1-3)Fe alloys. The β-transus temperature was found with an uncertainty of about ± 15 °C. A normal furnace and the heating rate of 10 °C/min used for DSC test. X-ray Diffractometer (BRUKER-D8) equipped with a 1-D (LYNXEYE) fast detector was used for phase analysis while Cu-Kα with a wavelength of 1.54060 Å was used as the x-ray source. The scans were performed with 0.025° step size, exposure time of 0.1 s/step and in the 2-theta (2θ) range of 29°–85°. The resulting patterns were analyzed using DIFFRAC.EVA V4.0 software.

The microhardness values of Ti6Al(1-3)Fe alloys were measured using a digital Micro-Vickers hardness tester (WOLPERT-Model: 401MVD) according to ASTM E 384 [16]. Microhardness measurements were conducted by a diamond indenter at a load of 1 kgf which applied on the randomly selected positions of each specimen at a dwell time of 10 s. Tensile tests were carried out using a 50 KN universal tensile testing machine (SHIMADZU) according to ASTM E8/E8M-13a [17]. In addition, the fracture surfaces of these specimens were microscopically examined using SEM. The average value of three different measurement of both hardness and tensile test was reported.

Electrochemical characterization was conducted using a standard three-electrode system at room temperature according to ASTM Standard G102-89 (2010) [18]. Silver chloride electrode (Ag/AgCl) was used as reference electrode while counter electrode was platinum (Pt) wire. The working electrode was Ti6Al(1-3)Fe alloy with an exposed working area of 1 cm^2 which was in contact to 3.5% NaCl solution as an electrolyte solution. All measurements were carried out using AutoLab PGSTAT128N potentiostat supported with Nova 1.11 software programme. During measurements, the potential of working electrode was continuously elevated from - 600 to + 600 mV at scan rate of 1 mV/s. The open circuit potential measurements were performed for a period of 28,800 seconds (8 h) at 1 mV/s scan rate. The corrosion rates were measured to identify the corrosion resistance of these alloys, using the linear polarization technique through the Tafel extrapolation method.

Results and Discussion

Microstructure Observation of Ti6Al(1-3)Fe Alloys

In the previous study of authors, it was found that the microstructure of Ti-6Al-4V alloy is referred as equiaxed which contain very fine equiaxed α- grains with an average size of 1.78 μm [19]. Ti6Al(1-3)Fe alloys are found that consist of a fully lamellar microstructure of α-plates in β-matrix as reported earlier [19]. The optical micrographs of Ti6Al(1-3)Fe alloys after thermo-mechanical treatment are illustrated in Fig. 2a–c. It can be observed that the lamellar colony size
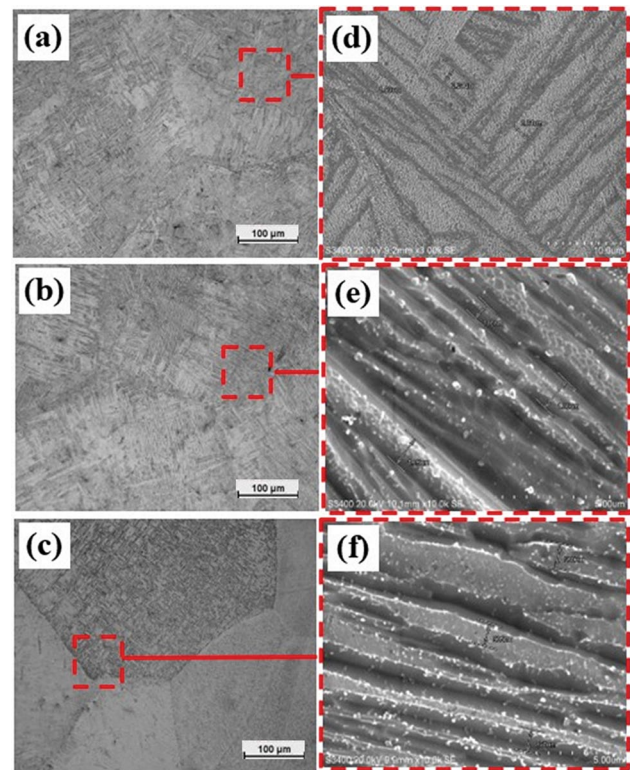

Fig. 2 The optical micrograph of Ti6Al(1-3)Fe alloys: **a** Ti6Al1Fe, **b** Ti6Al2Fe and **c** Ti6Al3Fe

and α-lamella width decrease by increasing Fe content. The average lamellar colony size of Ti6Al1Fe alloy is 780 μm which is larger than Ti6Al2Fe (644 μm) and Ti6Al1Fe (457 μm). In addition, the average lamella width of Ti6Al(1-3)Fe alloys decreases from 2.65 μm to less than 1 μm by increasing Fe content. FESEM micrographs of lamellar structure of Ti6Al(1-3)Fe alloys are also illustrated in Fig. 2d–f.

The DSC analysis of Ti6Al(1-3)Fe alloys was carried out to obtain β-transus (T$_\beta$) as shown in Fig. 3. The β-transus is the allotropic transformation temperature which plays a key role in thermomechanical/heat treatment processes. Depending on whether the alloy is processed or heat treated above or below T$_\beta$, different microstructures can be produced. The DSC curves corresponding to Ti6Al(1-3)Fe alloys reveal that T$_\beta$ varies in the small range between 1020 and 1050 °C which is higher than that of Ti-6Al-4V alloy (≈ 995 °C) which also determined using similar DSC conditions. According to literature, any small changes in concentration of Ti, Al, V results in changes in the β-transus and higher/lower β-transus is expected [20, 21]. The T$_\beta$ of Ti6Al(1-3)Fe alloys marginally decreases from 1050 °C to 1020 °C as Fe content increases indicating the solubility of Fe in the β-phase. It is suggested that Fe is a strong β-stabilizer alloying element which depresses the T$_\beta$. In addition, addition of Fe broadens the β-phase region.

**Fig. 3** DSC curves of Ti6Al(1-3)Fe alloys revealing the β-transus temperature
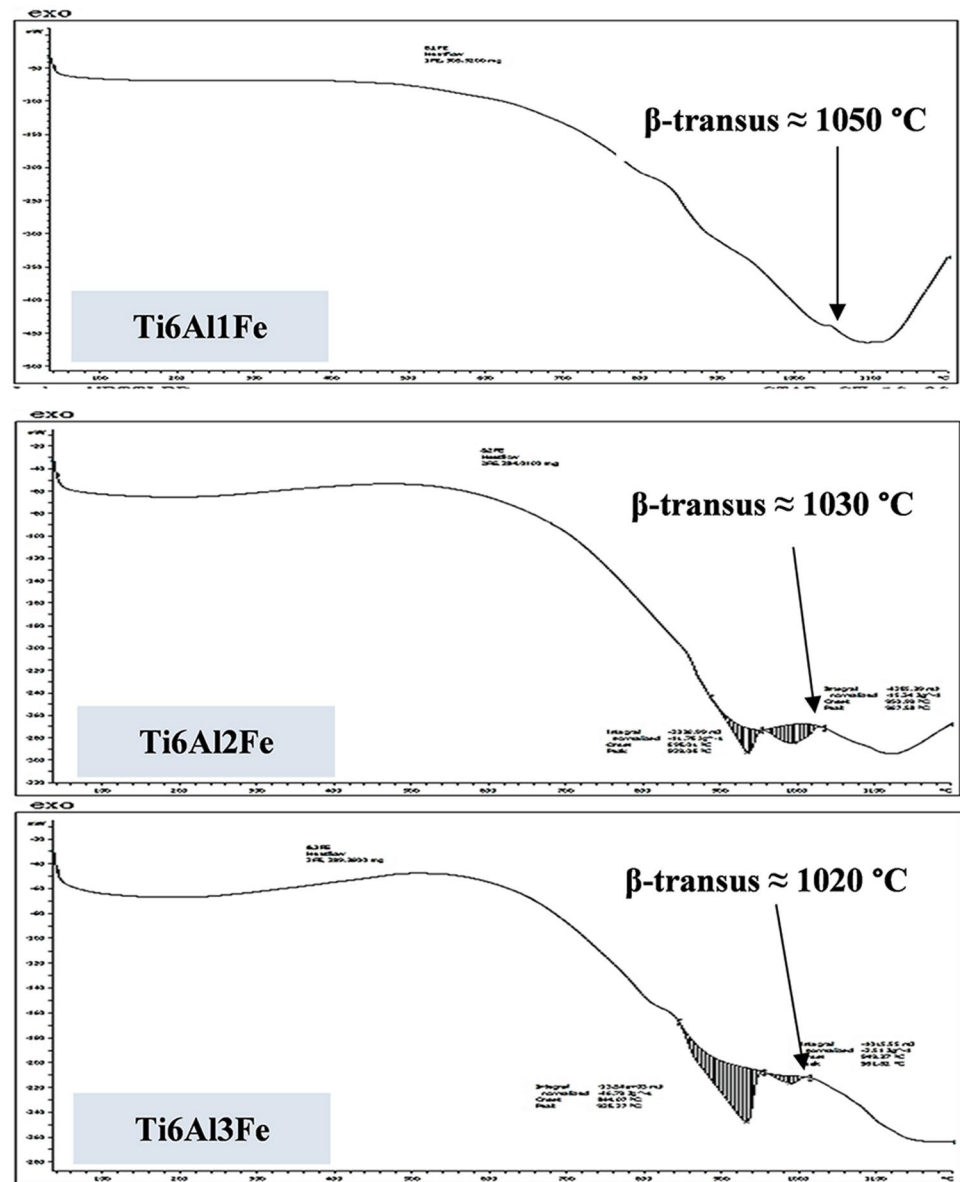
Ti6Al(1-3)Fe alloys subjected to hot rolling at 800 °C in the α+β phase region and solution heat treated at 900 °C below T_β followed by annealing at 900 °C. The microstructure of treated Ti6Al(1-3)Fe alloys is shown in Fig. 4. It can be observed that a bi-modal (α+β) microstructure is obtained from transformation of starting lamellar microstructures. The bi-modal (α+β) microstructures represent primary α-phase (α_p) and fine α lamellar colonies within a large β-phase matrix.

The microstructure of Ti6Al(1-3)Fe alloys after thermo-mechanical treatment exhibits differences in the size of α_p where grain size of α_p decreases by increasing Fe content. The average grain size of α_p in Ti6Al1Fe, Ti6Al2Fe and Ti6Al3Fe are 13.17, 10.90 and 8.60 μm, respectively. The decrease in the grain size of α_p is attributed to the average

lamellae's width of starting lamellar microstructures in each Ti6Al(1-3)Fe alloy before thermo-mechanical treatment as discussed previously. The grain size and the relative volume fraction of α_p phase are controlled by solution treatment parameters such as solution treatment temperature, holding time and cooling rate [22, 23].

A schematic physical model explaining the obtained bi-modal microstructure of Ti6Al(1-3)Fe alloys through thermo-mechanical treatment is presented in Fig. 5. The starting lamellar microstructure is transformed to bi-modal microstructure through the effect of hot rolling and heat treatment. Initially, the deformation of Ti6Al(1-3)Fe alloys during hot rolling at 800 °C in the α+β region results in distortion and fragmentation of most α-lamellae into globular shape while some non-distorted α-lamellae still remain in

Fig. 4 The optical micrograph of **a** Ti6Al1Fe, **b** Ti6Al2Fe and **c** Ti6Al3Fe after thermo-mechanical treatment
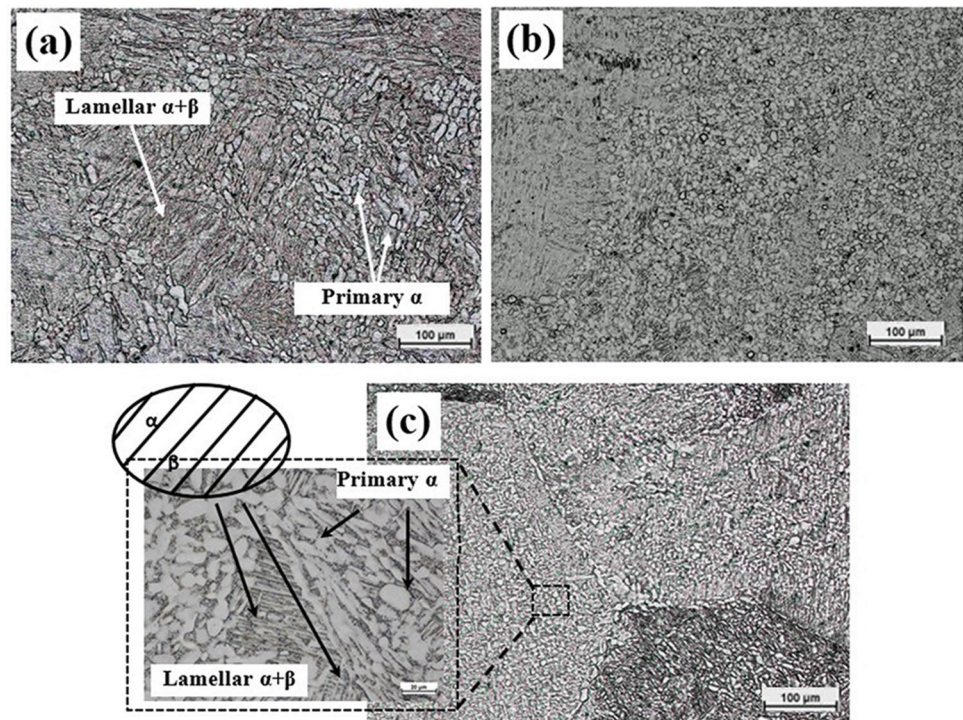
the microstructure. Ding *et al*. [22] have also reported the rotation of α-lamella and localized shear within hot deformation of Ti–6Al–4V alloy. The globular grains grow and convert into equiaxed grains due to the recrystallization of α-phase during the subsequent heat treatment until final bi-modal microstructure is stabilized. Thermo-mechanical process below T_β in the α+β region leads to recrystallization of α-phase and formation of equiaxed α-phase which referred as primary α (α_p) [22].

There are two possible mechanisms for fragmentation of α-lamellae; first formation of low and high angle boundaries across the alpha plates are formed and second occurring the localized shear and rotation of the α-lamella. In both cases, β-phase penetrates into α-lamella along these sub-boundaries or shear bands resulting in partial or fully fragmentation of α-lamella. By increasing Fe, the concentration of β-phase in the microstructure increases and further β-phase penetrates and accelerate the fragmentation of α-lamella. Besides, increasing Fe concentration reduces lamellae's width of starting lamellar and it also results in accelerated α-lamella fragmentation. Consequently, increasing Fe reduces the grain size of α_p. This mechanism of morphological changes and the developing of bi-modal microstructure from lamellar structure has also been reported elsewhere [22–26].

The XRD pattern of Ti6Al(1-3)Fe alloys subjected to thermo-mechanical treatment is illustrated in Fig. 6. XRD patterns clearly shows the separate peak associated with *hcp* α- and *bcc* β- phases revealing a dual phase microstructure

consist of coexistent α- and β-phases. The same phase constituents (α and β phases) can be found in all samples. By increasing Fe content (up to 3 wt%), the intensity of α peaks decreases, hence volume fraction of α phase increases. In contrast, the intensity of β phase peaks increases suggesting the increment of concentration of β phase. Strong β peaks can be noticed in Ti6Al3Fe as compared to others which exhibit more retention of β phase. Besides, the position of β phase basal peaks remains almost constant due to the limited solubility of Fe in Ti. XRD patterns also indicate the absence of any TiFe intermetallic compounds in the Ti6Al(1-3)Fe alloys, attributing to the presence of Fe as a strong β-stabilizer which suppress TiFe formation. Based on the XRD patterns, the volume fractions of α and β phases before and after thermo-mechanical treatment were estimated and listed in Table 1. It is obvious that the thermo-mechanical treatment leads to an increase in β- phase percentage. In addition, the percentage of β- phase increases as Fe content increases. Ti6Al3Fe has the highest amount of β phase of 17% while Ti6Al1Fe alloy has the lowest content of 10.1%. Thermo-mechanically treated Ti6Al(1-3)Fe alloys contain higher amount of β phase compared to un-treated alloys.

Mechanical Properties of Ti6Al(1-3)Fe Alloys

First of all, microhardness (HV) of Ti6Al(1-3)Fe alloys before and after thermo-mechanical treatment is investigated as tabulated in Table 2. Generally, thermo-mechanically

Fig. 5 Physical model showing the effect of thermo-mechanical process on the microstructure of Ti6Al(1-3)Fe alloys
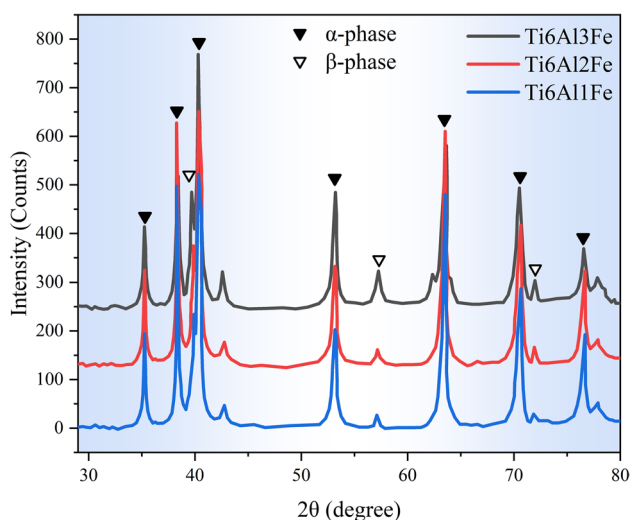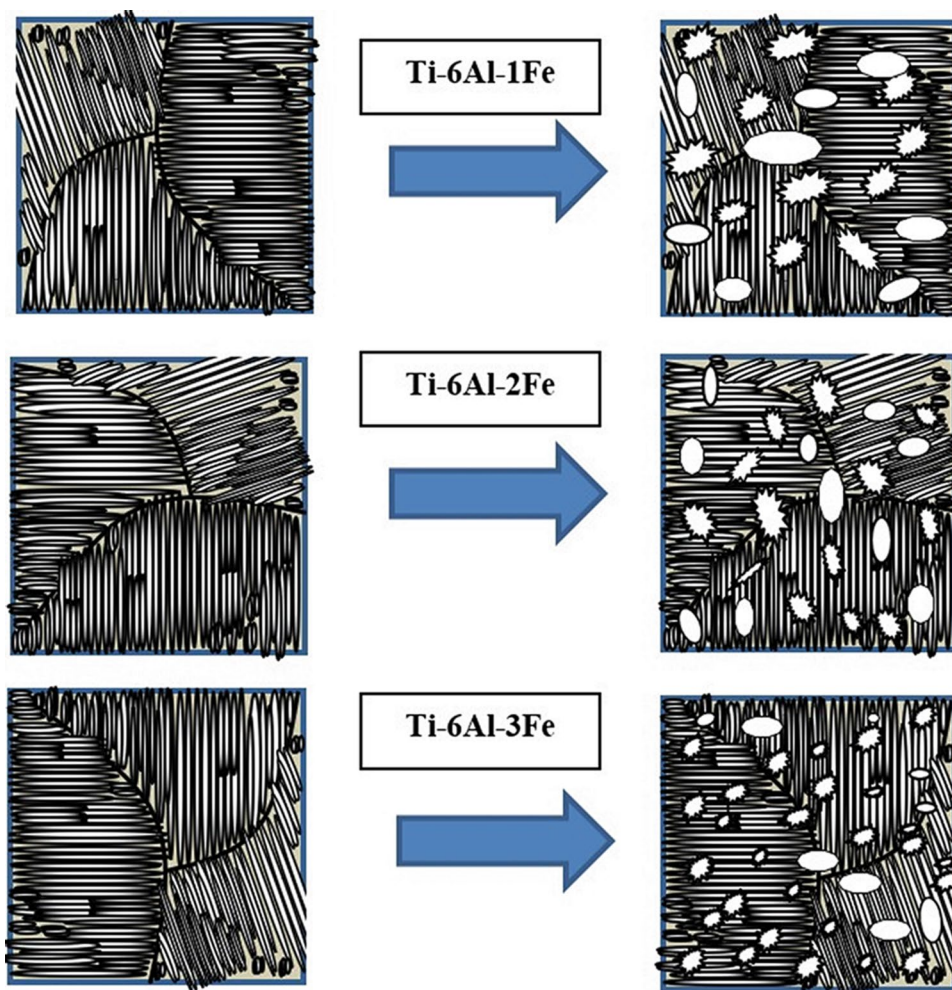

Fig. 6 XRD patterns of thermo-mechanical treated Ti6Al(1-3)Fe alloys

treated alloys have higher HV values relative to un-treated counterpart. In both un-treated and thermo-mechanically treated alloys, HV values increase by increasing Fe content where Ti6Al3Fe alloys show the highest HV values. It can be attributed to the refinement of microstructure by increasing Fe content as discussed in previous section. The maximum HV value of 464 HV was recorded for thermo-mechanically treated Ti6Al3Fe attributing to the refining of α_p in bi-modal ($\alpha+\beta$) microstructure. It was previously observed that the average grain size of α_p decreases from 13.17 to 8.60 µm by increasing Fe content.

The stress-strain curves of thermo-mechanically treated Ti6Al(1-3)Fe alloys is presented in Fig. 7. Thermo-mechanically treated alloys exhibit approximately typical elastic-plastic behaviour as observed in un-treated alloys. Thermo-mechanically treated alloys behave similarly in elastic region while they behave differently in plastic region in terms of ductility. The Ti6Al1Fe alloy displays more ductile behaviour while having higher tensile strength and ductility. Ti6Al1Fe and Ti6Al2Fe alloys display an offset from the ductile behaviour to a quasi-brittle. Figure 8 illustrates the

Table 1 The percentage of α and β phases in Ti6Al(1-3)Fe alloys before and after thermo-mechanical treatment

Phase Percentage (%)	Ti6Al1Fe		Ti6Al2Fe		Ti6Al3Fe	
	Before	After	Before	After	Before	After
α	91.9	65.6	89.6	56.6	86.9	48.0
β	8.1	10.1	10.4	13.2	13.1	17.0

Table 2 The mechanical properties of Ti6Al(1-3)Fe alloys before and after thermo-mechanical treatment

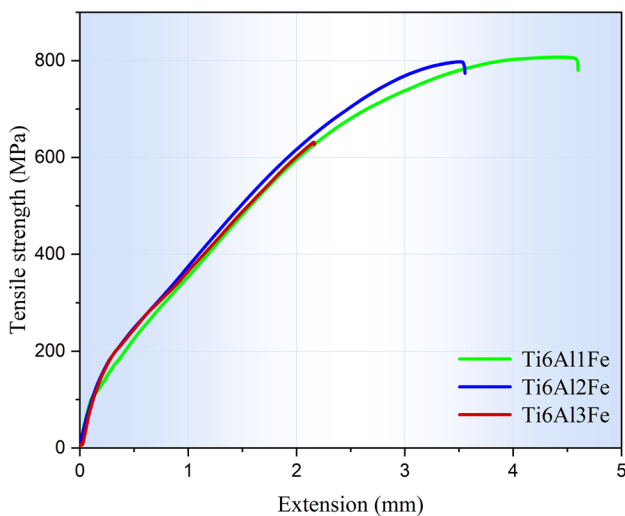|	Ti6Al1Fe		Ti6Al2Fe		Ti6Al3Fe	
	Before	After	Before	After	Before	After
HV	327 ± 5	414 ± 4	363 ± 4	442 ± 7	400 ± 8	464 ± 6
UTS	897 ± 6	808 ± 9	974 ± 4	798 ± 6	1069 ± 8	631 ± 5
Elongation (%)	11.3 ± 1.2	8.24 ± 0.8	10.4 ± 0.6	6.38 ± 0.9	8.1 ± 1.1	3.90 ± 0.4

Fig. 7 The stress-strain curve of thermo-mechanically treated Ti6Al(1-3)Fe alloys

fracture surfaces of thermo-mechanically treated Ti6Al(1-3) Fe alloys. The fracture surfaces of thermo-mechanically treated alloys are almost similar due to bi-modal (α+β) microstructure. Thermo-mechanically alloys exhibit a mixed ductile-brittle fracture mode. Some cleavages and microcracks are observed coupled with small dimples as a ductile fracture signature. Un-treated alloys also show a mixed ductile-brittle fracture is not shown here. In contrast, Ti-6Al-4V represent a fully ductile fracture mode.

The variations of ultimate tensile strength (UTS) and percentage of elongation (E%) are also presented in Table 2. In the case of un-treated alloys, UTS values increases by increasing Fe content where Ti6Al3Fe alloy has the highest UTS of 1069 MPa which is appeared at the expense of its ductility which declines to 8.1%. The ductility of un-treated alloys modestly decline with increasing

Fe content as expected. Ti6Al3Fe shows the lowest elongation percentage of 8.1% and then poorest ductility. The refined microstructure of Ti6Al(1-3)Fe increases HV and UTS values. The refinement of microstructure provides a large amount of dislocation within microstructure. According to Hall–Petch equation [27], the amount of stress (σ_y) required to transmit the dislocation through the boundary increases as the grain size become finer.

$$\sigma_y = \sigma_i + Kd^{-1/2}$$

where (σ_i) is the yield strength in the absence of grain boundaries (infinite grain size), (K) is the Hall–Petch constant, and (d) is the mean grain diameter. Therefore, finer lamellar microstructure of un-treated Ti6Al(1-3)Fe alloys restricts the dislocations movement and slip in the grains/ lamellae resulting in considerable increase in the HV and UTS values. Furthermore, the improvement of the HV and UTS values of un-treated alloys can be attributed to the presence of Fe atoms in interstitial positions of BCC lattice structure of β-phase. The dislocations which are understood to be the responsible source of plastic deformation are restrained to the Fe interstitial atoms (solutes) which hinder the dislocation movement and increase the mechanical properties.

Interestingly, a notable reduction in the UTS and ductility can be observed after thermo-mechanical process. Besides, the tensile strength and ductility gradually decreases as Fe content increases. It might be attributed to the applied excessive plastic deformation that lead to internal stress and appearing internal and surface cracks as showed in Fig. 8. The deterioration of strength properties appeared after thermo-mechanical treatment might be attributed to larger amount of β-phase and the titanium oxides that exist in a remarkable amount in the heat-treated alloys as found in XRD data.

Fig. 8 Typical fracture surfaces of thermo-mechanically treated Ti6Al(1-3)Fe alloys at different magnifications
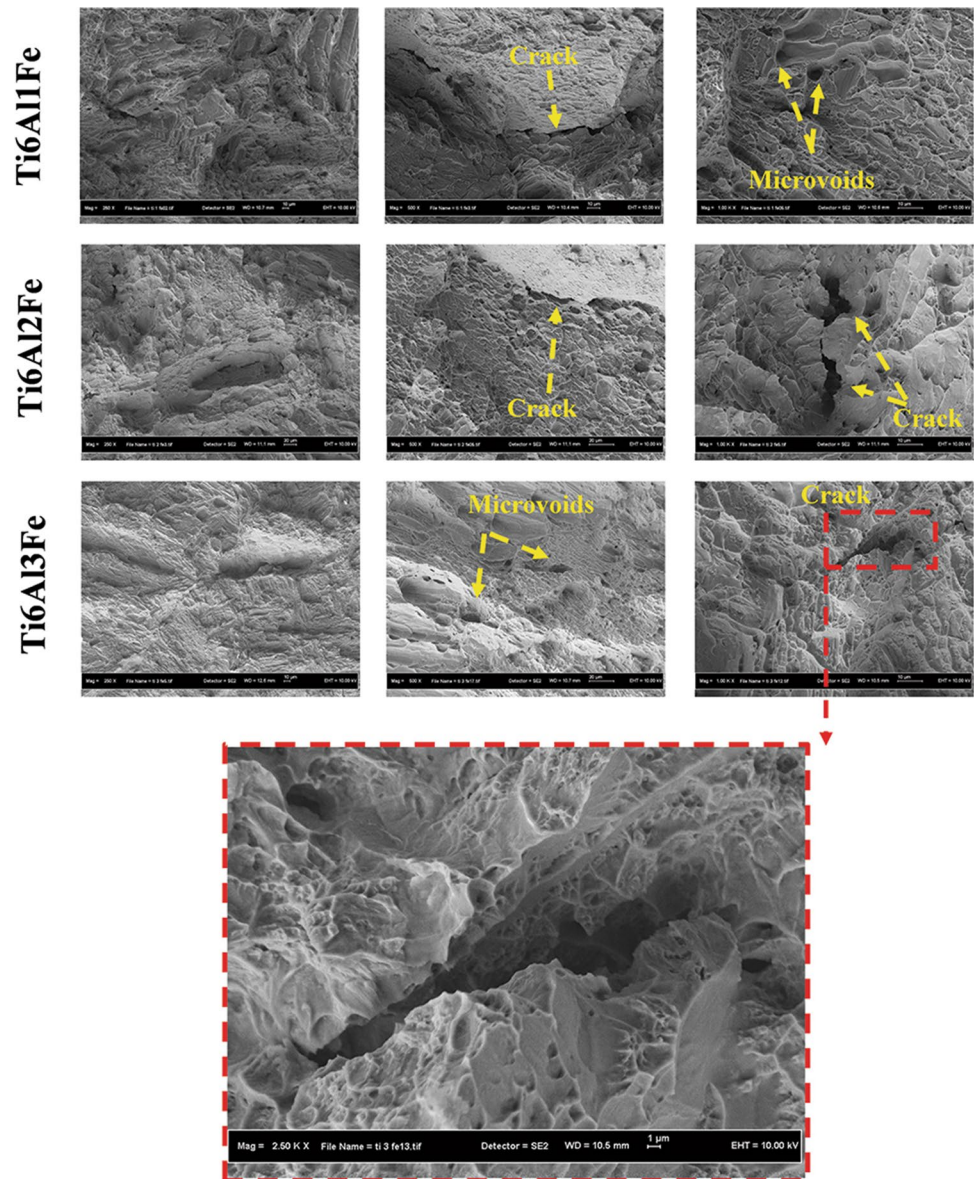
Corrosion Properties of Ti6Al(1-3)Fe Alloys

Figure 9 illustrates the OCP vs immersion time curve of thermo-mechanically treated Ti6Al(1-3)Fe alloys. It can be observed that the obtained OCP vs immersion time curves respond quite differently. In each specimen, the corrosion potential increases quickly within the first few minutes indicating spontaneous passivation due to formation of natural oxide film on specimens' surfaces. In Ti6Al1Fe alloy, the corrosion potential shift quickly toward the positive direction with the highest corrosion potential but after passing 14,000 second its behaviour changes considerably to the negative direction reaching the steady state at the lowest potential compared with Ti6Al2Fe and Ti6Al3Fe alloys.

On the other hand, corrosion potential of Ti6Al2Fe and Ti6Al3Fe alloys shifts toward positive values at different rates until the end of the experiment time at 8 h (28,800s) without reaching the steady state. According to Jiménez et al. [28], the OCP measurements could extend for a few days to reach the stability of the corrosion potential depending on the circumstances. This more positive or noble corrosion potential suggests the formation of a more stable protective film on the surface of specimens. Comparing the OCPs of thermo-mechanically treated Ti6Al3Fe alloys with that of un-treated alloys revealed that oxide films are formed more rapidly and more positive potential values.

Figure 10 depicts the potentiodynamic polarization curves for Ti6Al(1-3)Fe alloys. It can be seen that the electrochemical responses of these alloys are fairly similar while corrosion parameters are different. The corrosion parameters of the corrosion potential (E_{corr}) and the corrosion rate (C.R) calculated through extrapolation of
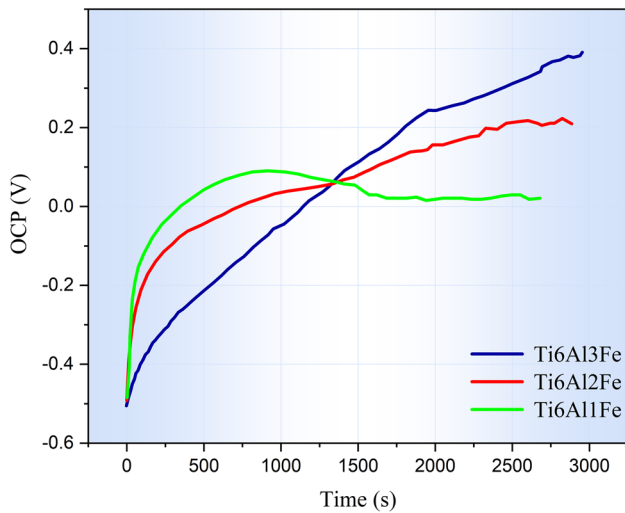
Fig. 9 The OCP vs time behaviour of treated Ti6Al(1-3)Fe alloys in 3.5%Nacl solution

Tafel plots are summarized in Table 3. In general, the un-treated alloys possess a better corrosion resistance compared with their counterpart thermo-mechanically treated alloys. It can be found that the un-treated alloys have a larger (nobler) E_{corr} than the thermo-mechanically treated ones. It is well known that a lower value of E_{corr} indicates the higher corrosion resistance [29]. This might be attributed to the larger percentage of α phase, which is nobler than β phase [30]. Besides, there is also a positive shift in E_{corr} values by increasing Fe content in both un-treated specimens. It suggests that, the corrosion resistance of Ti6Al(1-3)Fe alloys decreases with increasing Fe content. As observed in XRD results, the β-phase increases with increasing Fe-content which results in the reduction in corrosion resistant. Thermo-mechanically treated alloys show the largest E_{corr} of -391 mV and lowest corrosion resistance. Moreover, these results are completely compatible with the findings of OCP measurement in the previous section. Ti6Al1Fe alloy has the highest corrosion resistant.

Based on corrosion resistance class (CRC), it is worthy to mention that un-treated Ti6Al3Fe alloys can be classified as a perfectly stable materials in 3.5% NaCl solution, where their corrosion rates are less than 10^{-3} mm/year. The lowest corrosion rate of 1.77 E-05 mm/year belongs to Ti6Al1Fe alloy, while the highest corrosion rate of 2.29 E-05 was recorded by Ti6Al3Fe alloy. It can be inferred that the corrosion rate of un-treated alloys increases with increasing of Fe content. Thermo-mechanically treated specimens show higher corrosion rate than un-treated ones. the highest corrosion rate of 4.70E-05 was recorded by thermo-mechanically Ti6Al3Fe alloy.
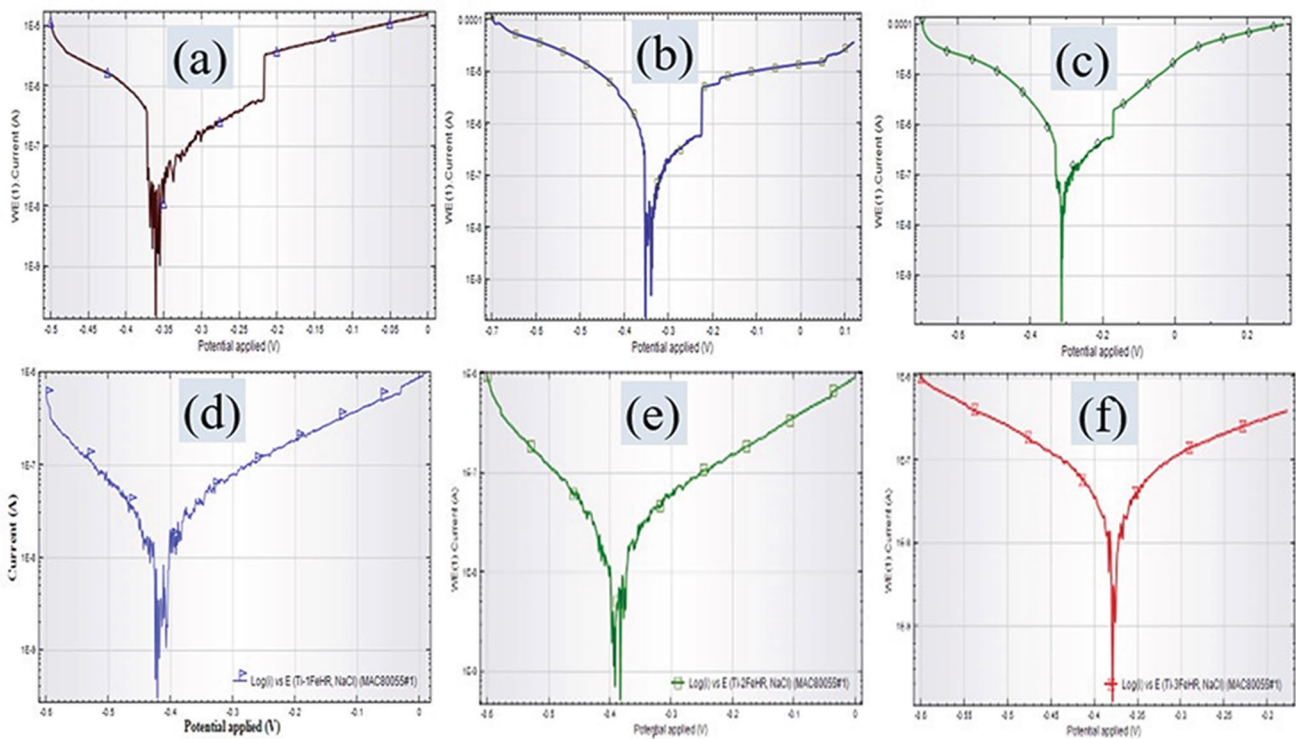

Fig. 10 The polarization curves of **a–c** un-treated and **d–e** thermo-mechanically treated Ti6Al(1-3)Fe alloys immersed in 3.5% NaCl Solution

Table 3 Corrosion parameters of Ti6Al(1-3)Fe alloys before and after thermo-mechanical treatment

	Ti6Al1Fe		Ti6Al2Fe		Ti6Al3Fe	
	Before	After	Before	After	Before	After
Corrosion Potentials (mV)	− 365	− 338.06	− 354	− 291.85	− 312	− 391.94
Corrosion Rate (mm/year)× 10^{-5}	1.77	2.27	2.09	3.21	2.29	4.70

Conclusions

Microstructural variation, mechanical and corrosion behavior of Ti6Al(1-3)Fe alloys after compositional modification and subsequent thermo-mechanical treatment was studied. The following conclusion were made as follows:

1. Ti6Al(1-3)Fe alloys contain a lamellar α+β microstructure wherein size of lamellar colonies and the lamellae width gradually decrease by increasing Fe content. The subsequent thermo-mechanical treatment lead to an increase in β-phase percentage wherein the percentage of β-phase increases by increasing Fe content.
2. Ti6Al(1-3)Fe alloys show a superior hardness, tensile strength and ductility owing to bi-modal α+β microstructure. The HV and UTS values of Ti6Al3Fe alloys increases by increasing Fe content attributing to the refined lamellar microstructure. HV values of Ti6Al(1-3)Fe alloys increase after thermo-mechanical treatment while UTS and elongation (%) values drop due to the increased amount of β-phase.
3. The corrosion resistance of Ti6Al(1-3)Fe decreases after thermo-mechanical treatment attributing to the larger content of β-phase which is susceptible to corrosion.

References

1. V. Vaithiyanathan, V. Balasubramanian, S. Malarvizhi, V. Petley, S. Verma, Combined effect of Gas Tungsten Arc Welding process variants and post-weld heat treatment on tensile properties and microstructural characteristics of Ti–6Al–4V Alloy joints. Metallogr. Microstruct. Anal. **9**, 194–211 (2020)
2. L. Wang, H. Ma, Q. Fan, J. Yao, X. Shen, S. Zhang, Y. Zhou, Y. Peng, Y. Gao, D. Wang, Simultaneously enhancing strength and ductility of Ti-6Al-4V alloy with the hierarchical structure via a novel thermal annealing treatment. Mater. Charact. **176**, 111112 (2021)
3. P.P. Singh, R.K. Gupta, V.A. Kumar, R.C. Gundakaram, S.K. Singh, Tailoring the microstructure and mechanical properties of titanium alloy Ti6Al4V forgings with different combinations of thermo-mechanical processing and heat treatment cycles. Trans. Indian Natl. Acad. Eng. **6**, 839–855 (2021)
4. C. Leyens, M. Peters, *Titanium and Titanium Alloys: Fundamentals and Applications* (Wiley, London, 2006)
5. J. Šmilauerová, J. Pospíšil, P. Harcuba, V. Holý, M. Janeček, Single crystal growth of TIMETAL LCB titanium alloy by a floating zone method. J. Cryst. Growth. **405**, 92–96 (2014)
6. Z. Liang, J. Miao, T. Brown, A.K. Sachdev, J.C. Williams, A.A. Luo, A low-cost and high-strength Ti-Al-Fe-based cast titanium alloy for structural applications. Scrip. Mater. **157**, 124–128 (2018)
7. H. Kadiri, L. Wang, H.O. Gulsoy, P. Suri, S. Park, Y. Hammi, R. German, Development of a Ti-based alloy: design and experiment. JOM. **61**, 60–66 (2009)
8. F. Hideki, T. Kazuhiro, Development of high performance Ti-Fe-Al alloy series. Nippon. Steel. Tech. Rep. **74**, 113–117 (2002)
9. A.O. Abdalla, A. Amrin, S. Muhammad, M.A.A. Hanim, Microstructures and hardness of newly designed Ti-6Al-(1–3)Fe alloys. Appl. Mech. Mater. **864**, 142–146 (2017)
10. A.O. Abdalla, A. Amrin, S. Muhammad, M.A.A. Hanim, Iron as a promising alloying element for the cost reduction of titanium alloys. A Review. Appl. Mech. Mater. **864**, 147–153 (2017)
11. Amrin, A. O. Abdalla, M. Toozandehjani, N. Abdul, microstructural transformation by compositional modification of Ti-6Al-4V alloy for aerospace applications. The International Professional Doctoral Symposium (iPDOCs'19), Universiti Teknologi Malaysia, Kuala Lumpur, Malaysia (2019).
12. A. Bahador, J. Umeda, R. Yamanoglu, A. Amrin, A. Alhazaa, K. Kondoh, Ultrafine-grain formation and improved mechanical properties of novel extruded Ti-Fe-W alloys with complete solid solution of tungsten. J. Alloy. Compound. **875**, 160031 (2021)
13. A. Bahador, A. Issariyapat, J. Umeda, R. Yamanoglu, C. Pruncu, A. Amrin, K. Kondoh, Strength-ductility balance of powder metallurgy Ti–2Fe–2W alloy extruded at high-temperature. J. Mater. Res. Technol. **14**, 677–691 (2021)
14. Q. Chao, P. Cizek, J. Wang, P.D. Hodgson, H. Beladi, Enhanced mechanical response of an ultrafne grained Ti-6Al-4V alloy produced through warm symmetric and asymmetric rolling. Mater. Sci. Eng. A. **650**, 404–413 (2016)
15. Y. Chong, T. Bhattacharjee, J. Yi, S. Zhao, N. Tsuji, Achieving bi-lamellar microstructure with both high tensile strength and large ductility in Ti–6Al–4V alloy by novel thermomechanical processing. Materialia. **8**, 100479 (2019)
16. ASTM E384-17, *Standard Test Method for Microindentation Hardness of Materials* (ASTM International, West Conshohocken, 2017)
17. ASTM E8/E8m-13a, *Standard Test Methods for Tension Testing of Metallic Materials* (ASTM International, West Conshohocken, 2013)
18. ASTM G102-89, *Standard Practice for Calculation of Corrosion Rates and Related Information from Electrochemical Measurements* (ASTM International, West Conshohocken, 2010)
19. A.O. Abdalla, A. Amrin, S. Muhammad, M.A.A. Hanim, Effect of heat treatment parameters on the microstructure and microhardness of Ti-6Al-4V alloy. AIP. Conf. Proc. **1865**, 030001 (2017)

20. R. Jing, S.X. Liang, C.Y. Liu, M.Z. Ma, X.Y. Zhang, R.P. Liu, Structure and mechanical properties of Ti–6Al–4V alloy after zirconium addition. Mater. Sci. Eng. A. **552**, 295–300 (2012)

21. O.M. Ivasishin, R.V. Teliovych, V.G. Ivanchenko, S. Tamirisakandala, D.B. Miracle, Processing, microstructure, texture, and tensile properties of the Ti-6Al-4V-1.55B eutectic alloy. Metallur. Mater. Trans. A. **39**, 402–416 (2007)

22. R. Ding, Z.X. Guo, A. Wilson, Microstructural evolution of a Ti–6Al–4V alloy during thermomechanical processing. Mater. Sci. Eng. A. **327**, 233–245 (2002)

23. D. Banerjee, J.C. Williams, Perspectives on titanium science and technology. Acta. Mater. **61**, 844–879 (2013)

24. M. Motyk, K. Kubiak, J. Sieniawski, and W. Ziaja, Hot plasticity of alpha beta alloys, in: A.K.M. Nurul Amin, Titanium alloys-towards achieving enhanced properties for diversified applications, 87-115. Intech. Open, (2012).

25. V.A. Joshi, *Titanium alloys: an atlas of structures and fracture features* (Taylor & Francis, New York, 2006)

26. T. Seshacharyulu, S.C. Medeiros, W.G. Frazier, Y.V.R.K. Prasad, Microstructural mechanisms during hot working of commercial grade Ti-6Al-4V with lamellar starting structure. Mater. Sci. Eng. A. **325**, 112–125 (2002)

27. C.E. Carlton, P.J. Ferreira, What is behind the inverse Hall-Petch effect in nanocrystalline materials? Acta. Mater. **55**, 3749–3756 (2007)

28. Y.S. Jiménez, M.T. Gil, M.T. Guerra, L. Baltes, J.M. Rosca, Interpretation of open circuit potential of two titanium alloys for a long time immersion in physiological fluid. Bull. Transilvania. Uni. Braşov. **51**, 197–204 (2009)

29. Y. Abdelrhman, M.A.H. Gepreel, S. Kobayashic, S. Okanoc, T. Okamoto, Biocompatibility of new low-cost ($\alpha+\beta$)-type Ti-Mo-Fe alloys for long-term implantation. Mater. Sci. Eng. C. **99**, 552–562 (2019)

30. J. Yang, H. Yang, H. Yu, Z. Wang, X. Zeng, Corrosion behavior of additive manufactured Ti-6Al-4V alloy in NaCl solution. Metallur. Mater. Trans. A. **48**, 3583–3593 (2017)

Authors and Affiliations

Ayad Omran Abdalla[1] · Astuty Amrin[2] · Khairur Rijal Jamaludin[2] · Meysam Toozandehjani[3]

✉ Astuty Amrin
  Astuty@utm.my

1 College of Mechanical Engineering Technology, Alrahba Street, Alfwayhat, Benghazi, Libya

2 Razak Faculty of Technology and Informatics, Universiti Teknologi Malaysia Kuala Lumpur, 54100 Jalan Semarak, Kuala Lumpur, Malaysia

3 New Technologies Research Center, Amirkabir University of Technology, Tehran Polytechnic, 424 Hafez Ave., P.B. 15875-4413, Tehran, Iran